Polímeros
ISSN 1678-5169 (Online)

https://doi.org/10.1590/0104-1428.20220013

ORIGINAL ARTICLE

Polymer composite produced with Brazil nut residues and high impact polystyrene

Jefferson Renan Santos da Silva[1], João Christian Paixão Fonseca[1], Thais da Silva Santos[1], Josiel Bruno de Oliveira[1], Thiago Monteiro Maquiné[2], Bruno Mello de Freitas[1], Raimundo Nonato Alves Silva[1], Nayra Reis do Nascimento[1], João Martins da Costa[1], Roger Hoel Bello[1] and José Costa de Macedo Neto[1*]

[1]Departamento de Engenharia de Materiais, Universidade do Estado do Amazonas – UEA, Manaus, AM, Brasil

[2]Programa de Pós-graduação em Ciência e Engenharia de Materiais – PPGCEM, Universidade Federal do Amazonas – UFAM, Manaus, AM, Brasil

**jmacedo@uea.edu.br*

Abstract

Solid residues from agroindustry often accumulate and cause environmental imbalance. An alternative to this is to use this residue as a reinforcement in polymers. The achievement of this work was to characterize a composite with a polystyrene matrix reinforced with Brazil nut shells residues. The residues were cleaned and ground to then produce the samples via injection molding with the proportions of 0%, 2.5% and 5% of load. The specimens were characterized using mechanical tensile testing and thermogravimetric analysis (TGA). The mechanical test showed that the composite with 2.5% of filler had greater stiffness and strength was improved by 5%. Thermal analysis showed an increase in the temperature for the beginning of the degradation of the M2.5 composite. The results confirm a potential application in the automotive industry for the polystyrene composite reinforced with Brazil nut shells.

Keywords: *residues, polystyrene, HIPS, characterization.*

How to cite: Silva, J. R. S., Fonseca, J. C. P., Santos, T. S., Oliveira, J. B., Maquiné, T. M., Freitas, B. M., Silva, R. N. A., Nascimento, N. R., Costa, J. M., Bello, R. H., & Macedo Neto, J. C. (2022). Polymer composite produced with Brazil nut residues and high impact polystyrene. *Polímeros: Ciência e Tecnologia*, *32*(4), e2022038. https://doi.org/10.1590/0104-1428.20220013

1. Introduction

The Brazil nut (*Bertholletia excelsa*), one of the tree species of greatest economic importance in the Amazon region, has excellent quality wood, but felling of these trees is prohibited. Its fruit, which is a husk with the nuts inside, has natural rigidity and is part of the extractive activities of the Amazon[1]. Brazil nut trees have great economic value due to the exploration of their nuts (which have about 60 to 70% lipids and 15 to 20% proteins)[2].

In Brazil, the state of Amazonas stands out for being the largest producer of Brazil nuts, and production was 11,707 tonnes in 2020, which is equivalent to 35.3% of the total produced in the country[3]. However, studies show that, for every ton of shelled nuts, 1.4 tons of residues are produced, which are composed of the shells and the husks[4]. One of the solutions to the problem of the accumulation of residues that is currently being investigated is the use of plant waste as a filler in polymeric composite materials and other so-called traditional engineering materials[5]. In this context, the management of residues benefits organizations and society through the commercialization of these materials and the generation of income through the practice of recycling and sustainability[6]. In addition, the alternative use of lignocellulosic materials, such as Brazil nut shells, either as particles or fibers in polymer composites, has been studied due to factors such as increased elastic modulus and mechanical strength, in addition to reducing the weight and cost of the final product[7].

Polystyrene (PS) at room temperature is an amorphous glassy polymer and has low energy absorption under impact due to the absence of local mobility of chain segments, since its Tg occurs between 90 and 100 C. Obtaining rubber-PS results in the product known as high impact polystyrene (HIPS), which under impact has mechanical properties that are superior to PS. This improvement is mainly due to the introduction of a flexible amorphous component (Tg ≤ - 40 °C) in the rigid matrix of PS[8].

An important polymer that can be used in composite materials with shell residues as a filler is high impact polystyrene (HIPS). This polymer consists of a multiphase copolymer in which rubber particles of polybutadiene (PB) are dispersed in the rigid matrix of polystyrene (PS). HIPS has a melting temperature (T_m) of 180-270 °C, and is usually processed via injection at 210 to 260 °C, and its main application is in electronic components[9]. In addition to its temperature

not being high during processing, these characteristics make HIPS of great interest for applications in composites with lignocellulosic materials, since the optimization of the balance of rigidity and impact properties can be achieved by controlling the morphology and formulation of the composite[10].

In the literature, studies using Brazil nut shells have already obtained promising results[11]. Some other studies have produced polymeric composites using lignocellulosic fillers obtained from agricultural tailings and HIPS matrix and polystyrene. Zafar and Siddiqui[12] produced polymeric composites by *in situ* polymerization with a polystyrene matrix using rice husk, wheat husk and mustard husk as fillers. In this study, the husks were ground to 250-355 µm, 355-500 µm, and 500-710 µm. The authors performed the tensile test in which composites with a wheat husk and mustard husk filler of 250-235 µm at 10% load achieved better results, while the composite with rice husk of 355-500 µm achieved a better result with a 5% load. Siregar et al.[13] produced a composite with HIPS and pineapple fiber with and without alkaline treatment. The composites were prepared using an intensive mixer and then the mixture was hot pressed in a compression mold. The fibers were ground and passed through a sieve with a 10-40 mesh. The authors tested the melt flow index (MFI) and observed that the melt flow index of the composite with untreated fiber was 0.316 g/10 min, while that of neat HIPS was 4.0 g/10 min.

Saber et al.[14] produced a composite by compression molding using a HIPS matrix and filler made up of sugarcane bagasse in the quantities of 10, 20, 30, 40, 50% with treatments in water, HCl, NaOH solution and oil. The results were interpreted by bar graph comparison. All composites using water-treated fibers reduced tensile strength and increased elastic modulus in relation to pure HIPS. Composites with 10 to 20% wt/wt fibers reduced 32% tensile strength, those with 30 to 40% wt/wt reduced 40% and 50% wt/wt showed a 60% reduction. Additionally, all composites increased the elastic modulus above 20% in relation to pure HIPS, and the composite with 50% wt/wt fiber showed an increase of 250%. The treatments of the composites with 5% HCl, 5% NaOH and oil increased Young's modulus by an average of 20% for all the composites relative to pure HIPS. The tensile strength was reduced by an average of 55% for all composites compared to pure HIPS. In our work, we show the mechanical and thermal performance of a HIPS composite with a Brazil nut shell filler obtained from Amazonian agro-industry. For this, the materials were produced via injection molding, and is one of the very few works on HIPS with Brazil nut shells.

Thus, the objective of this work was to produce a polymeric composite material using a HIPS matrix and Brazil nut shells as the lignocellulosic filler. Obtaining this material aims at possible applications in the automotive industry since it combines lower weight and high rigidity. Due to this application, it is necessary to understand the fracture mechanism of this composite, as HIPS presents deformation by microfibrillation or crazing and the shell acts as a filler that increases rigidity. A large majority of the literature shows the crazing in a two-dimensional manner with a large shortcoming since the propagation of the crazing is not shown in 3 dimensions, but this is addressed in this work. For this, a detailed study of the basic fracture mechanism of the tensile test was performed using optical and scanning electron microscopy (SEM). Finite element simulations were also performed to obtain the thermal transient behavior in the material, in addition to the characterizations using FT-IR, TGA and DSC.

2. Materials and Methods

2.1 Aquisition and cleaning of residues and aquisition of high-impact polystyrene

The Brazil nut shells were obtained from a producer in the Amazonas state, Brazil. Figure 1a shows the tree that provides the nut shells that can be used as a filler in plastics. Figure 1b-1c show the fruit, in this case, the open husk and inside it the nuts can be seen. Inside the shells are the white-colored nuts. Figure 1 d shows the shells left after removing the nuts. These residues were used to obtain the polymeric composite materials.

After collection, manual scraping and dry brushing were performed to remove any residue[10]. Subsequently, the shells were ground using a knife mill (MA048 Marconi). Finally, the ground shells were sieved through a 20 mesh sieve (Tyler/ABNT). The particle dimensions were measured using a digital optical microscope (VHX-100, Keyence, Japan) and presented dimensions (between 1.0-2.39 mm). The HIPS used as the matrix was donnated by INNOVA, Manaus.

2.2 Production of composites

The sample was obtained using injection moulding in which the HIPS was weighed and separated into two different quantities, taking as a reference the value of 0.7500 kg as the maximum amount of material. The proportion was defined in relation to its weight being 2.5% (M2.5) and

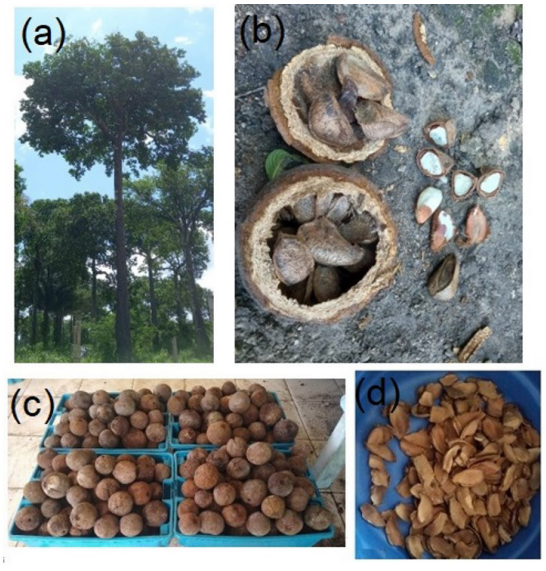

Figure 1. (a) Brazil nut tree (*Bertholletia excelsa*); (b-c) the husk, which is the fruit obtained from the tree; (d) residues from the shells of the nuts. Photos: author, 2021.

5% (M5) of residue. A storage container was used to mix the shells in particulate form and the HIPS in pellet form. Mixing was performed manually by preparing the container, seeking to ensure the best mixing of the polymer matrix and filler. This method was used because it is practical and fast, and is economical because it does not add another process, such as extrusion, in order to mix the polymer and filler[15]. For the production of samples according to the ASTMD 638-2010 standard, an injection moulding machine (300/1400/390 CL, Krauss Maffei, Germany) was used. The temperatures of the zones were 200 °C (T1), 228 °C (T2), 225 °C (T3) and 238 °C (T4). For the injection process, a speed of 75 mm/s was used, and injection pressures of 900 bar, relief pressure of 800 bar, injection time 5 s, relief time of 15 s and cooling time of 30 s.

2.3 Characterization

For the characterization, an FT-IR spectrometer (Nicolet 6700 Madison, Thermo Scientific, USA) was used. The measurements were made in ATR (germanium crystal) mode using the FT-IR Imaging Microscope (Nicolet Continuun Madison, Thermo Scientific, USA). The ranges used were between 4,000-675 cm^{-1} and the resolution was 4 cm^{-1} and the SCAN number was 64. The samples were analyzed via tensile testing on the universal testing instrument (Series 5980, Instron, USA). Tensile testing was carried out according to the ASTMD 638-2010 standard with type I sample dimensions, 150 kN cell, test speed 5.0 mm/s, and 3 samples were tested. Scanning electron microscopy (SEM) (Vega3, Tescan) with a voltage of 10 kV was used to analyze the faces of the fractures obtained in the tensile tests. The TG analysis was performed in a TGA-DSC thermogravimetric analyzer (TGA-50M Shimadzu, Japan), with the aid of a microanalytical scale (MX5, MetllerToledo, Switzerland). The method used was the TGA021, which consists of heating from 25 °C to 600 °C, at the rate of 10 °C/min, under an inert atmosphere of nitrogen (50 mL/min). This analysis was applied to the residue, the HIPS and the composites. The glass transition temperature is the temperature at which the polymeric chains of the amorphous phase acquire mobility. To determine the glass transition (Tg) temperatures, a differential scanning calorimeter (DSC) (DSC1, Mettler Toledo, Switzerland) was used in the temperature range from -30 to 300 °C, heating rate of 10 K/min, under an atmosphere of N_2 with a flow rate of 50 mL/min. To study the thermal transient and predict some of the mechanical properties of the composites and HIPS, finite element analysis (FEA) was used. For this analysis, Ansys Workbench® software was employed. In this simulation, heat was applied to the end of the sample, as seen in Figure 2. The simulation started at 25 °C and an external temperature of 50 °C, which, according to Saber et al.[14], is the maximum operating temperature for HIPS, for 8 h in the transient regime.

The material type, explicit dynamic mode and characteristics of a quasi-static test were obtained from the Ansys® software library. The contour parameters used in the software for the HIPS analysis were a) displacement of |100| mm (tensile), b) analysis time of $7x10^{-4}$ s, c) mesh size of 3 mm, d) 257 knots, e) 219 elements and f) Poisson coefficient of 0.407. The outline properties for the HIPS were a density of 1.021 $kg.m^3$, thermal expansion coefficient of 84 C^{-1}, elastic modulus of 737.17 MPa, melt modulus of 8.19 x 10^8 Pa, shear modulus of $2.73x10^8$ Pa, flow voltage of 14.22 MPa, isotropic thermal conductivity of 0.12 $W.m^{-1}.C^{-1}$ and specific heat of 0.23 $J.g^{-1}.K^{-1}$. The specific heat (Cp) represents the energy required to change the temperature of a unit of mass of the material by one degree. The following Equation 1 was used in the thermal transient simulation (temperature and time variation)[16].

$$\nabla^2 + \frac{\dot{q}}{k} = \frac{1}{\alpha}\frac{\partial T}{\partial t} \quad (1)$$

Where:

$\dot{q}$ = heat generation as a function of time;

$\alpha = \frac{k}{\rho c}$ = thermal diffusivity of the material;

k = thermal conductivity of the material;

ρ = specific mass;

c = specific heat;

$\frac{\partial T}{\partial t}$ = temperature variation over time;

$\nabla^2 T$ = thermal gradient.

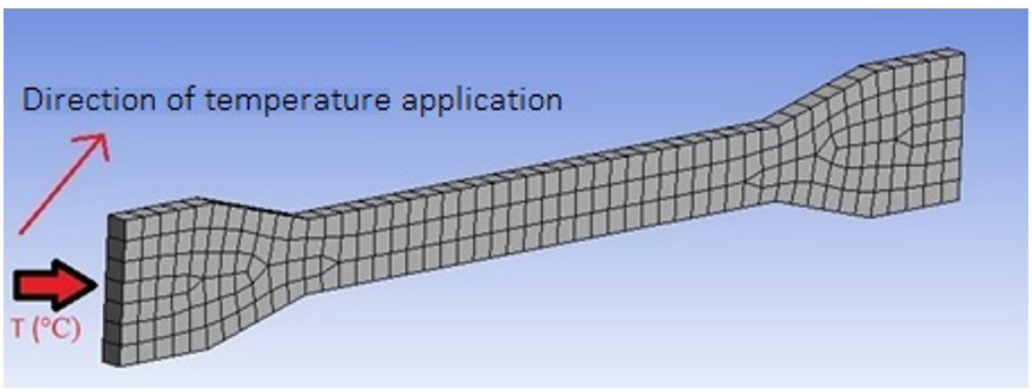

Figure 2. Direction of temperature application in the sample.

3. Results and Discussion

Figure 3 illustrates the infrared spectrum for the Brazil nut shell residue, HIPS polymer (0%) and the polymer composites of the HIPS matrix containing 2.5% (M2.5) and 5% (M5) of Brazil nut shells. According to Figure 3, it is possible to observe that the spectrum of the Brazil nut has two intense absorption bands at 3,424 cm^{-1}, which are related to O-H bond stretching. Close to 1,742 and 1,615 cm^{-1}, the stretching bands (C=O) are observed, which are attributed to carboxylic acids and esters. For lignin, these stretchings have been associated with aliphatic ketones and substituted aromatic ketones, respectively. Additionally, the band at 1,615 and 1,374 cm^{-1} corresponds to aromatic skeleton vibrations, which are characteristic of lignin, while the bands at 1,453, 1,374 and 1,315 cm^{-1} are related to deformation (C-H). Finally, close to 1,160 cm^{-1}, the C-O stretching occurs and, at 1,104 and 1,056 cm^{-1}, the deformation of OH of the C-OH group occurs[17].

In relation to the spectrum of the HIPS polymer, it is possible to observe five main bands in Figure 3. The bands between 3,400-2,700 cm^{-1} are related to axial deformation in the hydrogen atoms attached to the carbon, oxygen and nitrogen atom (C-H, C-O and N-H). In the regions between 3,080-3,020 cm^{-1}, it is possible to observe the bands representing the C-H vibrations of the alkenes. In addition, the two absorption bands of the region between 2960-2850 cm^{-1} represent aliphatic C-H (primary and secondary carbons). The absorption bands between 1,600-1,450 cm^{-1} are the vibrations of the C=C band of aromatic carbons[18].

In relation to the composites using the HIPS polymer with the reinforcement of 2.5 (M2.5) and 5% (M5) Brazil nut shells, it is possible to verify the presence of all the main bands of the neat HIPS polymer, as previously reported. It was not possible to verify significant alterations in the spectra; however, it is important to note in Figure 3 that there is an increase in the band close to 1,500 cm^{-1} (C=C aromatic symmetric stretching for lignin), which may be associated with an increase in the lignin content present in composites[19].

The results of the tensile test can be seen in Table 1, while the image of the sample after the tensile test is shown in Figure 4. It is observed that, after adding the residues, the material showed a considerable increase in the properties of average maximum stress, yield stress and elastic modulus compared to the neat polymer, thus making it more rigid.

HIPS has a glassy matrix of polystyrene that is rigid due to its chemical structure that it contains aromatic rings as a pendant group. The incorporation of a second elastomeric phase in a PS vitreous matrix has as a main objective the increase in its toughness, i.e., its impact resistance[20]. The addition of a rigid material tends to increase the rigidity

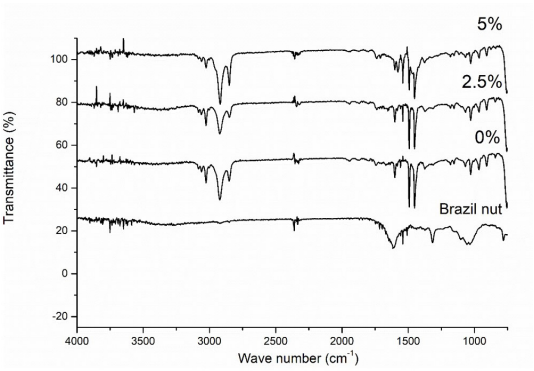

Figure 3. FT-IR spectra for Brazil nut shells, HIPS composites with different concentrations of Brazil nut shells.

Table 1. Results of the mechanical tests of neat polymer and composites.

Sample	Tensile strength (MPa)	Elongation (%)	Elastic modulus (GPa)
HIPS	23.19±0.54	37.40±0.22	0.86±0.03
M2.5	20.51±0.54	11.66±0.48	0.85±0.02
M5	21.64±0.07	7.30±1.97	0.89±0.02

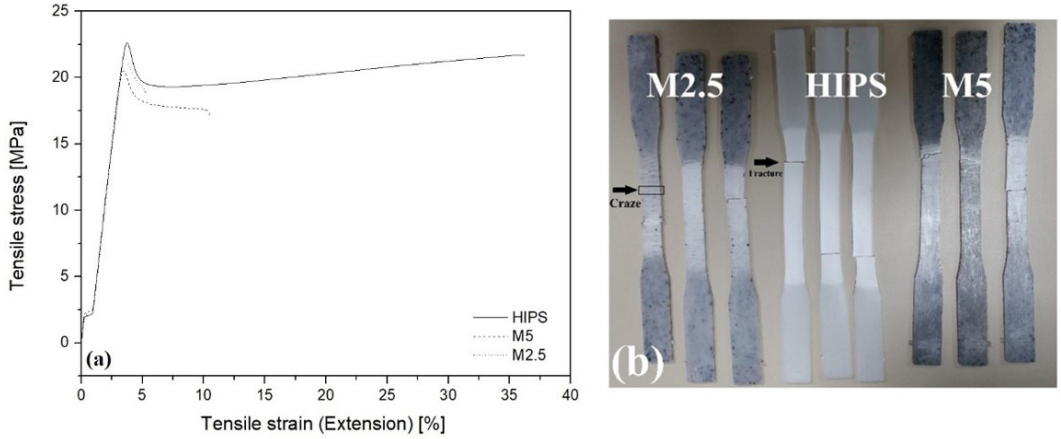

Figure 4. (a) tension-deformation curves of samples after the tensile test; (b) fractures in the samples after the tensile test.

of the composite because, when there is a greater amount of reinforcement, up to a limit value so that it can be covered by the matrix, it will contribute to the greater strength of the composite. Furthermore, fillers reduce the free movement of polymer chains, thus resulting in an increase in their elastic modulus[21,22]. According to Table 1, the tensile strength of M5 was higher (21.64 MPa±0.07) compared to M2.5 (20.51 MPa±0.54). This occurred because as the fiber content increases, the stresses become more evenly distributed and the composite strength increases[23,24]. However, M5 had a higher elastic modulus (0.89 GPa±0.02) than M5 (0.85 GPa±0.02). The values of the means of the elastic modulus are close, and the difference between them is not statistically significant.

A study was carried out of the fractures of the test samples tested after the tensile test, and is illustrated in Figure 4a-4b. Figure 4a shows the behavior of the stress deformation curves for HIPS and the composites. It can be observed in Figure 4b that the behavior of the fractures showed it to be brittle and all the fractures occurred in the useful area of the samples. HIPS is composed of two immiscible phases of polybutadiene and polystyrene. The introduction of an elastomeric phase in the rigid PS matrix, as expected, promotes a decrease in the elastic modulus value, which means that the tenacified material deforms at stresses lower than those verified for the PS homopolymer[25].

The presence of blanching in all the samples is also observed. This blanching is called microfissuring or crazing and ais formed by 50% of the highly oriented polymers and 50% of the voids, which causes the process of dilatational deformation[26]. These microfissures occur in amorphous polymers, such as polystyrene, and are characterized by a whiteness of the amorphous region, due to differences in the refractive index that causes light scattering of the fibrils in the crazing[27]. It is observed in Figure 4b that the presence of crazing is perpendicular to the main stress in the tensile test. The stress at the tip of the crazing is greater than the average stress of the tension in the material; thus, the crazing tends to grow in the direction that is perpendicular to the uniaxial main stress in the tensile test[28].

Although the crazing is formed in all the samples, it can be observed in Figure 4b that the crazing formed in HIPS is less intense than that formed in the composites. This implies that the rubber microparticles in the HIPS induced the formation of crazing around them[29]. The growth of crazing is interrupted and restarted when it finds another rubber particle providing the emergence of smaller crazes[30]. These smaller cracks allowed a greater dissipation of applied energy before the catastrophic cracks and this caused a greater elongation in relation to the composites[26].

Figure 5b reveals that the composites demontrated a lower elongation than the HIPS, and the M5 composite showed a lower elongation when compared to M2.5.

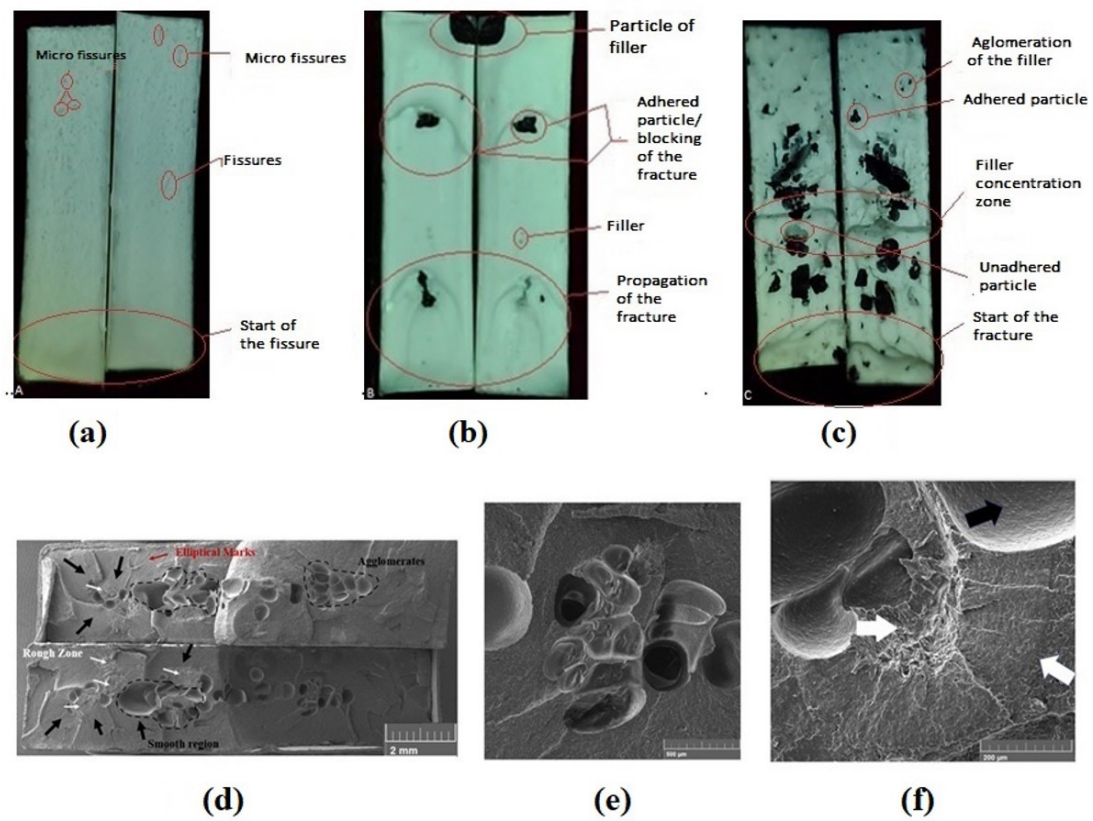

Figure 5. Digital optical microscope images of fracture faces: (a) HIPS; (b) M2.5; (c) M5. Scanning electron microscopy: (d) fracture face of M5 composite with magnification at 21x; (e) region of clusters with magnification at 150x; (f) surfaces of clusters with magnification at 440x.

The shell particles acted as stress concentrators and, as M5 has a greater amount of shell, therefore it became more fragile and has less elongation[31]. Another reason is that the rubber particles influenced a weakening in the adhesion of the fiber-matrix interface, thus preventing the mechanical anchoring of the polystyrene molecules on the surface of the shells, further weakening the composites[32].

Figure 5a-5c shows the fracture faces of the HIPS, and the M2.5 and M5 composites, respectively. Figure 5a shows the presence of micro fissures in the fracture of the HIPS. In Figure 5b, it can seen that the Brazil nut shell particles act as a stress concentrator at the end of the propagation of the elliptical-shaped crack[33]. However, in Figure 5c, it is observed that the greater amount of shell increased the stress concentrators, further weakening the composite, which is proven by the reduction of elongation.

Figure 5d-5f shows the scanning electron microscopy image of a fracture in the composite M5. Figure 5d shows the face of the fracture side by side after the tensile test. In the image, it is possible to observe that the shells tended to agglomerate in the matrix of HIPS and become stress concentrator points[11]. It is also possible to observe the smooth regions (black arrows) that propagated towards the clusters by shear and are perpendicular to the tensile stress[31]. Few elliptical regions (red arrow) are observed[34]. Figure 5f shows the presence of unstuck shells and regions that derive from the weak interaction of the matrix and the shell. In Figure 5f, a roughness is observed on the surface of the region that pulled the shell out of the matrix. This roughness is a result of the small rubber balls that are scattered in the HIPS matrix. In the figure, it is also possible to observe a fibrillar region (white arrow), which is characteristic of a catastrophic fracture. It is also possible to observe the division (white arrow) of the region that presented a fast and a slow craze propagation speed[35].

In Figure 6a-6b, the thermogravimetric curves of the Brazil nut shells and the HIPS are presented. While in Figure 6c-6d, the thermogravimetric curves of the composites M2.5 and M5 are presented. Additionally, in Table 2, there is a summary of the temperatures and respective weight loss of the samples studied, i.e., filler (Brazil nut shells), neat polymer and its composites. It is important to note that the average mass of the samples was 10.20±0.11 mg.

The DTG curve of the residue showed that, at a temperature of 73.56 °C, there was a 1.391 mg loss of moisture (13.7%) due to the lignocellulosic materials having a hydrophilic character, as already cited by Viana et al.[10]. Subsequently, there was a considerable weight loss of about 5.39 mg (53.08%) at 371.8 °C, which is related to the decomposition of the cellulose through the endothermic process. Finally,

Table 2. Thermal results of the filler, HIPS and its composites.

Sample	Thermal events	Decomposition temperature (°C)	Weight loss (%)	Residue (%)
Filler	1st	73.56	13.710	33.209
	2nd	371.80	53.081	
HIPS	1st	444.68	100.184	
	-		-	0.1%
M2.5	1st	427.24	98.556	
	-		-	1.444
M5	1st	275.94	83.092	6.626
	2nd	428.40		

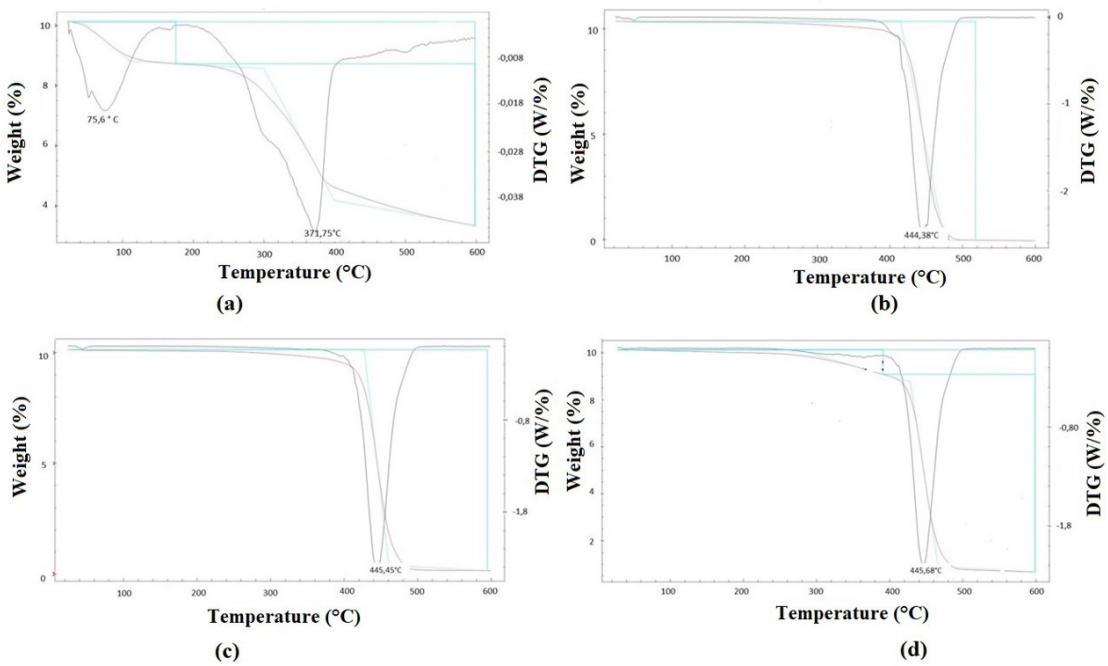

Figure 6. TGA results: (a) TG (red) and DTG (black) of filler; (b) TG (red) and DTG (black) of neat HIPS; (c) TG (red) and DTG (black) of M2.5 composite; (d) TG (red) and DTG (black) of M5 composite.

the weight loss at the end of the analysis was 6.78 mg (66.79%), which can be attributed to lignin degradation[36].

The HIPS curves showed a single stage of mass loss at approximately 444.88 °C, which is also the level observed in the works of Cordeiro et al.[37] and Agung et al.[38]; in this case 415 °C. The curves of the composites showed that the addition of the residue provided a slight increase in the temperature at the beginning of degradation of the M2.5 composite, i.e., 444.68 °C (Figure 6c), but for the M5 composite this temperature dropped to 275.94 °C (Figure 6d).

After the analysis of TGA, it was observed that the shells presented a residue of 33% by weight. Neat HIPS presented a residue of 0.1% by weight. While the composites M2.5 and M5 obtained a residue of 1.444% and 6.262%, respectively. The HIPS sample almost totally decomposed in the analysis (about 0.1%). The addition of filler in the HIPS polymer matrix of resulted in residues at the end of the analysis for both compositions, which were more expressive at 5% of filler, indicating the presence of the Brazil nut shells.

Figure 7 illustrates the DSC thermograms for neat HIPS polymer and the composites. According to Figure 7, peaks around 90 °C are attributed to moisture absorbed by the shells[39]. Additionally, it can be observed that the Tg of the composites did not show significant alterations in relation to the neat HIPS, and varied between 100 and 103 °C. This small alteration in the Tg can be attributed to the restriction imposed by the shells to the molecular movement of the HIPS matrix[40]. Figure 7 also shows the specific heat (Cp) reduction for composites. This behavior was caused by the shells, which reduced heat transfer[38]. The shells of Brazil nuts consist of the exotesta regions, central mesotesta region, mesotesta vascular region and tegmen that present structures with voids such as long and porous cells, porosities and vascular exchanges[41,42]. These voids can be filled with air and moisture that act as resistance to heat transfer reducing the Cp for composites[43,44].

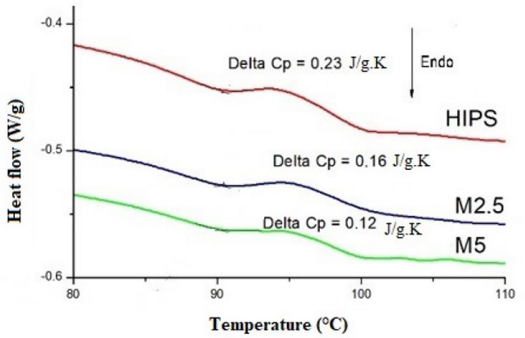

Figure 7. DSC thermograms for neat HIPS and for the composites M2.5 and M5.

In order to verify the thermal transient behavior of the composites with M2.5, M5 and the HIPS, a simulation was performed using Ansys® Workbench software. The parameters used in the simulation, such as specific heat Cp of composites M2.5, M5 and HIPS were obtained from the DSC analysis (Figure 7), i.e., $C_{pM2.5}$: 0.16J/g.K, C_{pM5}: 0.12 J/g.K and C_{pHIPS}: 0.23 J/g.K.

After the simulations, the software provided the images of the thermal transient behavior of the composites and HIPS and these can be seen in Figure 8a-8c. From the images, it is possible to observe that the composites obtained a higher thermal resistance than the HIPS during the period of 8 h (288 s). The addition of the lignocellulosic shells and the lack of a coupling agent effectively slowed the heat transfer in the HIPS matrix[44,45].

Figure 9 shows the graph obtained from the final minimum temperature after simulation for neat HIPS polymer and the composites. According to Figure 9, it is possible to observe that the HIPS left the initial equilibrium state after 288 s at 25.001 °C and, after 8 h in operation, the minimum temperature in the sample was 44.831 °C. The M2.5 composite, tested under the same conditions as the HIPS, showed greater resistance at the initial temperature

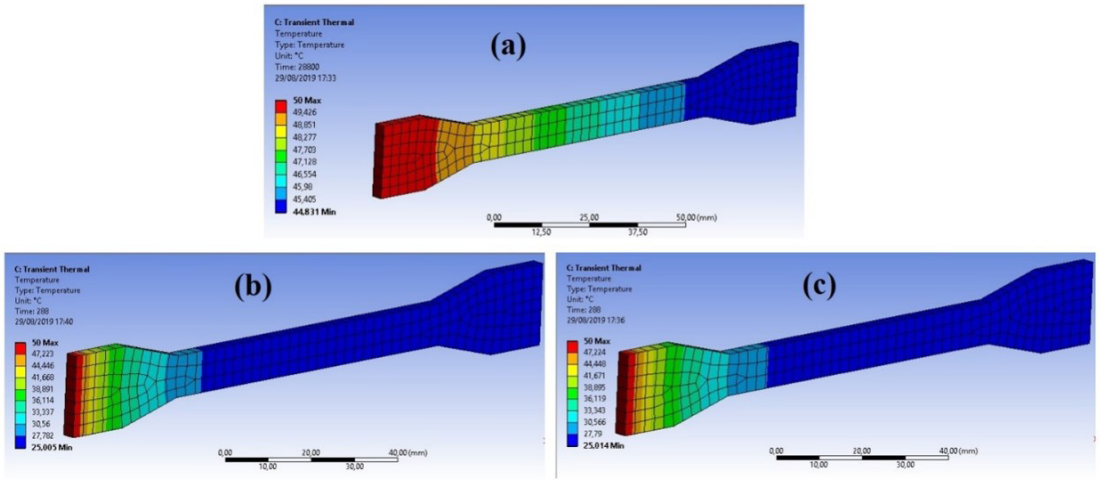

Figure 8. Temperature propagation in the materials: (a) HIPS; (b) M2.5; (c) M5.

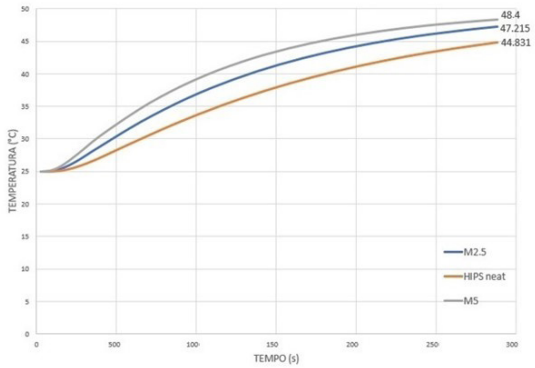

Figure 9. Final minimum temperature of the virtual test.

of 25.005 °C and, at the end of the 8 hours in operation, the minimum temperature in the sample was 47.215 °C. This represents a higher temperature; approximately 5% higher when compared to HIPS. The M5 composite started the thermal transition at 25.014 °C, and showed a higher initial thermal resistance when compared to the other two materials (HIPS and M2.5), however, at the end of the 8 hours, the minimum temperature in the sample was 48,400 °C. This implies an approximately 8% higher temperature when compared to the HIPS and the M2.5 composite.

The technique of producing the composite using the injection molding process has shown that it is possible to obtain the products quickly. The values for tensile strength and elastic modulus of HIPS and composites were close, but the elongation reduced for composites in relation to HIPS. The addition of filler in the HIPS caused an increase in thermal resistance (thermal insulation). This behavior has shown that the application in the production of automotive parts is possible.

4. Conclusions

In this study we investigated the role of Brazil nut shells in the thermal and mechanical properties of high impact polystyrene polymer (HIPS) and HIPS-based composites. According to the mechanical properties, it can be said that, after the addition of 2.5 and 5% by mass of the Brazil nut residues, there were no significant changes in the values obtained for the elastic modulus and tensile strength. The values were similar to those obtained for the pure HIPS polymer of 0.85 GPA and 23 MPa, respectively. However, for ductility, there was a progressive decrease in values after the increase in the amount of residues. The residues have high values of lignin and hemicellulose that hinder adhesion with the polymer matrix, justifying a superficial chemical treatment. Additionally, the results of the scanning electron microscopy corroborate the presence of agglomerates in the composites. Regarding the thermal properties, it is important to emphasize that the Brazil nut residues did not affect the thermal stability as well as the glass transition temperature values, as the values of both composites (M2.5 and M5) were similar to the pure polymer. Finally, the results demonstrated the potential suitability of the HIPS composite reinforced with Brazil nut residues, which could be a use for a residue that has little utility.

5. Author's Contribution

- **Conceptualization –** NA.
- **Data curation –** NA.
- **Formal analysis –** NA.
- **Funding acquisition –** NA.
- **Investigation –** Jefferson Renan Santos da Silva; João Carlos Martins da Costa; Roger Hoel Bello; José Costa de Macedo Neto; Raimundo Nonato Alves Silva; Nayra Reis do Nascimento.
- **Methodology –** Jefferson Renan Santos da Silva; João Carlos Martins da Costa; José Costa de Macedo Neto; João Christian Paixão Fonseca; Thais da Silva Santos; Josiel Bruno de Oliveira; Thiago Monteiro Maquiné; Bruno Mello de Freitas.
- **Project administration –** Jefferson Renan Santos da Silva; José Costa de Macedo Neto.
- **Resources –** NA.
- **Software –** NA.
- **Supervision –** José Costa de Macedo Neto.
- **Validation –** NA.
- **Visualization –** NA.
- **Writing – original draft –** Jefferson Renan Santos da Silva; João Martins da Costa; Roger Hoel Bello; José Costa de Macedo Neto.
- **Writing – review & editing –** Jefferson Renan Santos da Silva; João Martins da Costa; Roger Hoel Bello; José Costa de Macedo Neto.

6. Acknowledgements

We would like to thank the Amazonas State University (UEA), the Federal University of Amazonas (UFAM), the Research and Development Laboratory at UEA, and TESCAN Group for SEM images.

7. References

1. Nogueira, I. M. S., Lahr, F. A. R., & Giacon, V. M. (2018). Development and characterization of particleboards manufactured with the residue of Brazilian nut fruit and castor oil polyurethane resin. *Revista Matéria*, *23*(1), 1-11.
2. Souza, T. A. Fo., Pedroso, E. A., & Paes-de-Souza, M. (2011). Produtos Florestais Não-Madeiráveis (PFNMs) da Amazônia: uma visão autóctone da cadeia-rede da castanha-da-amazônia no estado de Rondônia. *Revista de Administração e Negócios da Amazônia*, *3*(2), 58-74.
3. Instituto Brasileiro de Geografia e Estatística – IBGE. (2020). *Extração vegetal e silvicultura*. Retrieved in 2022, December 02, from https://cidades.ibge.gov.br/brasil/am/pesquisa/16/0?tipo=ranking&indicador=12716
4. Bouvie, L., Bortella, D. R., Porto, P. A. O., Silva, A. C., & Leonel, S. (2016). Physico-chemical characterization of fruit's castanheira of Brazil. *Nativa*, *4*(2), 107-111. http://dx.doi.org/10.14583/2318-7670.v04n02a10.

5. Mansor, M. R., Mastura, M. T., Sapuan, S. M., & Zainudin, A. Z. (2019). *The environmental impact of natural fiber composites through life cycle assessment analysis*. In M. Jawaid, M. Thariq & N. Saba (Eds.), *Durability and life prediction in biocomposites, fibre-reinforced composites and hybrid composites* (pp. 257-285). Duxford: Woodhead Publishing. http://dx.doi.org/10.1016/B978-0-08-102290-0.00011-8.
6. Brasil. *Lei n. 12.305, de 2 de agosto de 2010*. (2010, 2 de agosto). Institui a Política Nacional de Resíduos Sólidos; altera a Lei nº 9.605, de 12 de fevereiro de 1998; e dá outras providências. Diário Oficial da República Federativa do Brasil, Brasília.
7. Borsoi, C., Scienza, L. C., Zattera, A. J., & Angrizani, C. C. (2011). Obtainment and characterization of composites using polystyrene as matrix and fiber waste from cotton textile industry as reinforcement. *Polímeros: Ciência e Tecnologia*, *21*(4), 271-279. http://dx.doi.org/10.1590/S0104-14282011005000055.
8. EnríquezMedrano, F. J., Acuña, P., & Morales, G. (2020). Synthesis strategies in the preparation of high impact polystyrene with diferent type of particles as the dispersed phase, towards a balance between impact strength and gloss. *Brazilian Journal of Chemical Engineering*, *37*(4), 715-727. http://dx.doi.org/10.1007/s43153-020-00040-y.
9. *INNOVA*. (2021, May 30). Retrieved in 2022, December 02, from https://www.innova.com.br/wp-content/uploads/2022/12/HIPS.pdf
10. Vianna, W. L., Correa, C. A., & Razzino, C. A. (2004). The effects of the high impact polystyrene morphology on the properties of wood-plastic composites. *Polímeros: Ciência e Tecnologia*, *14*(5), 339-348. http://dx.doi.org/10.1590/S0104-14282004000500012.
11. Petrechen, G. P., & Ambrósio, J. D. (2016). *Preparation and mechanics characterization of lignocellulosic residues of Brazil nut (bertholletia excelsa) seed husks reinforced polypropylene composites*. In *22º CBECiMat - Congresso Brasileiro de Engenharia e Ciência dos Materiais* (pp. 2739-2749). São Paulo: Metallum Congressos Técnicos e Científicos.
12. Zafar, F. M., & Siddiqui, M. A. (2018). Raw natural fiber reinforced polystyrene composites: effect of fiber size and loading. *Materials Today: Proceedings*, *5*(2), 5908-5917. http://dx.doi.org/10.1016/j.matpr.2017.12.190.
13. Siregar, J. P., Sapuan, S. M., Rahman, M. Z. A., & Zaman, H. M. D. K. (2009). The effect of compatibilising agent and surface modification on the physical properties of short Pineapple Leaf Fibre (PALF) reinforced High Impact Polystyrene (HIPS) composites. *Polymers & Polymer Composites*, *17*(6), 379-384. http://dx.doi.org/10.1177/096739110901700606.
14. Saber, E., El-Sayed, N. S., Nagiebb, Z. A., Ismail, A., & Kamel, S. (2017). Characterization of plastic composite based on HIPS loaded with bagasse. *Egyptian Journal of Chemistry*, *60*(6), 1101-1110.
15. Kieling, A. C., Santana, G. P., Santos, M. C., Macedo, J. C. No., Pino, G. G., Santos, M. D., Duvoisin, S. Jr., & Panzera, T. H. (2021). Wood-plastic composite based on recycled polypropylene and Amazonian tucumã (Astrocaryum aculeatum) endocarp waste. *Fibers and Polymers*, *22*(10), 2834-2845. http://dx.doi.org/10.1007/s12221-021-0421-3.
16. AZO Materials. (2001). *High Impact Polystyrene – HIPS*. Retrieved in 2022, December 02, from https://www.azom.com/article.aspx?ArticleID=424
17. Vieira, D. S., & Coelho, N. A. (2020). Utilização do método dos elementos finitos no estudotérmico de elementos simples de concreto. *Revista de Ciencia y Tecnología*, *6*, 1-16.
18. Pawlak, Z., & Pawlak, A. S. (1997). A review of infrared spectra from wood and wood components following treatment with liquid ammonia and solvated electrons in liquid ammonia. *Applied Spectroscopy Reviews*, *32*(4), 349-383. http://dx.doi.org/10.1080/05704929708003319.
19. Masood, M. T., Heredia-Guerrero, J. A., Ceseracciu, L., Palazon, F., Athanassiou, A., & Bayer, I. S. (2017). Superhydrophobic high impact polystyrene (HIPS) nanocomposites withwear abrasion resistance. *Chemical Engineering Journal*, *322*, 10-21. http://dx.doi.org/10.1016/j.cej.2017.04.007.
20. Troedec, M., Sedan, D., Peyratout, C., Bonnet, J. P., Smith, A., Guinebretiere, R., Gloaguen, V., & Krausz, P. (2008). Influence of various chemical treatments on the composition and structure of hemp fibres. *Composites. Part A, Applied Science and Manufacturing*, *39*(3), 514-522. http://dx.doi.org/10.1016/j.compositesa.2007.12.001.
21. Rovere, J., Correa, C. A., Grassi, V. G., & Pizzol, M. F. (2008). Caracterização morfológica do poliestireno de alto impacto (HIPS). *Polímeros: Ciência e Tecnologia*, *18*(1), 12-19. http://dx.doi.org/10.1590/S0104-14282008000100007.
22. Tobón, A. E. D., Chaparro, W. A. A., & Rivera, W. G. (2014). Improvement of properties of tension in WPC of LDPE: HIPS/natural fiber through crosslinking with DCP. *Polímeros: Ciência e Tecnologia*, *24*(3), 291-299.
23. D'Almeida, J. R. M. (1987). Propriedades mecânicas de fibras de juta. *Ciência e Cultura*, *39*(4), 1025-1032.
24. Joseph, K., Medeiros, E. S., & Carvalho, L. H. (1999). Tensile properties of unsaturated polyester composites reinforced by short sisal fibers. *Polímeros: Ciência e Tecnologia*, *9*(4), 136-141. http://dx.doi.org/10.1590/S0104-14281999000400023.
25. Medeiros, V. N. (2016). *Desenvolvimento de membranas de poliétersulfona por inversão de fases* (Doctoral thesis). Universidade Federal de Campina Grande, Campina Grande.
26. Grassi, V. G., Forte, M. M. C., & Pizzol, M. F. (2001). Morphologic aspects and structure-properties relations of high impact polystyrene. *Polímeros: Ciência e Tecnologia*, *11*(3), 158-168. http://dx.doi.org/10.1590/S0104-14282001000300016.
27. Rabelo, M., & Paoli, M.-A. (2013). *Aditivação de termoplásticos*. São Paulo: Artliber Editora.
28. Maestrini, C., Monti, L., & Kausch, H. H. (1996). Influence of particle-craze interactions on the sub-critical fracture of core-shell HIPS. *Polymer*, *37*(9), 1607-1619. http://dx.doi.org/10.1016/0032-3861(96)83709-8.
29. Argon, A. S. (2011). Craze initiation in glassy polymers - revisited. *Polymer*, *52*(10), 2319-2327. http://dx.doi.org/10.1016/j.polymer.2011.03.019.
30. Ebewele, R. O. (2000). *Polymer science and technology*. Boca Raton: CRC Press. http://dx.doi.org/10.1201/9781420057805.
31. Zhu, L. D., Yang, H. Y., Cai, G. D., Zhou, C., Wu, G. F., Zhang, M. Y., Gao, G. H., & Zhang, H. X. (2013). Submicrometer-sized rubber particles as "craze-bridge" for toughening polystyrene/high-impact polystyrene. *Journal of Applied Polymer Science*, *129*(1), 224-229. http://dx.doi.org/10.1002/app.38716.
32. Bhilat, H., Hachim, A., Salmi, H., & Had, K. (2020). Experimental and numerical investigation of the influence of temperature on the fracture behavior of high impact polystyrene evaluated by the J-integral approach using multiple specimen method. *Journal of Metals, Materials and Minerals*, *30*(3), 91-100. http://dx.doi.org/10.55713/jmmm.v30i3.763.
33. Şahin, T., Sınmazçelik, T., & Şahin, S. (2007). The effect of natural weathering on the mechanical, morphological and thermal properties of high impact polystyrene (HIPS). *Materials & Design*, *28*(8), 2303-2309. http://dx.doi.org/10.1016/j.matdes.2006.07.013.
34. Hasegawa, H., Ohta, T., Ito, K., & Yokoyama, H. (2017). Stress-strain measurement of ultra-thin polystyrene films: film thickness and molecular weight dependence of crazing stress. *Polymer*, *123*, 179-183. http://dx.doi.org/10.1016/j.polymer.2017.07.018.

35. Capri, M. R., Santana, L. C., & Mulinari, D. R. (2016). *Avaliação das propriedades térmicas dos compósitos de polipropileno reforçados com fibras da palmeira*. In *22º CBECiMat - Congresso Brasileiro de Engenharia e Ciência dos Materiais*. (pp. 1-12). São Paulo: Metallum Congressos Técnicos e Científicos..
36. Machado, C. E. V., Costa, A. C. A., Cardoso, R. C., Caetano, F. P., Lopes, J. A., Cury, A. L., Rodrigues, L. M., & Cabral, R. F. (2017). Study of mechanical and thermal properties of high impact polystyrene. *Cadernos UniFOA*, *12*(35), 15-24. http://dx.doi.org/10.47385/cadunifoa.v12.n35.474.
37. Cordeiro, C. C., Arroyo, P. A., Santos, D. G., Pedrini, C. No., Muniz, E. C., Radovanovic, E., & Rubira, A. F. (2005). *Blendas de poliestireno de alto impacto pós consumo com um resíduo plástico gerado em usina de reciclagem*. In *8º Congresso Brasileiro de Polímeros – CBPol* (pp. 699-700). São Carlos: Associação Brasileira de Polímeros.
38. Agung, E. H., Sapuan, S. M., Ahmad, M. M. H. M., Zaman, H. M. D. K., & Mustofa, U. (2011). *Differential scanning calorimetry (DSC) analysis of abaca fibre (Musa textile Nee) reinforced high impact polystyrene (HIPS) composites*. In P. Wang, L. Ai, Y. Li, X. Sang & J. Bu (Eds.), *Advanced materials research* (Vol. *295-297*, pp. 929-933). Zurich: Trans Tech Publications, Ltd. http://dx.doi.org/10.4028/www.scientific.net/AMR.295-297.929.
39. Saeed, U., Dawood, U., & Ali, A. M. (2021). Cellulose triacetate fiber-reinforced polystyrene composite. *Journal of Thermoplastic Composite Materials*, *34*(5), 707-721. http://dx.doi.org/10.1177/0892705719847249.
40. Scussel, V. M., Manfio, D., Savi, G. D., & Moecke, E. H. S. (2014). Stereoscopy and scanning electron microscopy of Brazil nut (Bertholletia excelsa H.B.K.) Shell, brown skin, and edible part: part one—healthy nut. *Journal of Food Science*, *79*(7), H1443-H1453. http://dx.doi.org/10.1111/1750-3841.12502. PMid:24974969.
41. Scussel, V. M., Manfio, D., Savi, G. D., & Moecke, E. H. S. (2014). Stereo and scanning electron microscopy of in-shell Brazil nut (Bertholletia excelsa H.B.K.): part two—surface sound nut fungi spoilage susceptibility. *Journal of Food Science*, *79*(11), H2392-H2403. http://dx.doi.org/10.1111/1750-3841.12679. PMid:25318846.
42. Liu, K., Takagi, H., & Yang, Z. M. (2011). Effect of lumen size on transverse thermal conductivity of unidirectional natural fiber-polymer composite via finite element method. *Materials Science Forum*, *675-677*, 431-434. http://dx.doi.org/10.4028/www.scientific.net/MSF.675-677.431.
43. Zach, J., Slávik, R., & Novák, V. (2016). Investigation of the process of heat transfer in the structure of thermal insulation materials based on natural fibres. *Procedia Engineering*, *151*, 352-359. http://dx.doi.org/10.1016/j.proeng.2016.07.389.
44. Ju, L., Yang, J., Hao, A., Daniel, J., Morales, J., Nguyen, S., Andrei, P., Liang, R., Hellstrom, E., & Xu, C. (2018). A hybrid ceramic-polymer composite fabricated by co-curing lay-up process for a strong bonding and enhanced transient thermal protection. *Ceramics International*, *44*(10), 11497-11504. http://dx.doi.org/10.1016/j.ceramint.2018.03.211.
45. Sottos, N. R., & Swindeman, M. (1995). Transient thermal deformations of the interphasein polymer composites. *The Journal of Adhesion*, *53*(1-2), 69-78. http://dx.doi.org/10.1080/00218469508014372.

Received: Feb. 16, 2022
Revised: Aug. 15, 2022
Accepted: Dec. 02, 2022